Group Sparsity Based Multi-Target Tracking in Passive Multi-Static Radar Systems Using Doppler-Only Measurements

Saurav Subedi, Yimin D. Zhang, *Senior Member*, *IEEE*, Moeness G. Amin, *Fellow*, *IEEE*, and Braham Himed, *Fellow*, *IEEE*

***Abstract*—In this paper, we consider the problem of tracking multiple targets in a passive multi-static radar system using Doppler-only measurements. The number of targets is assumed unknown and time-varying. The Doppler measurements are subject to additive noise, clutter, and missed detections. Doppler-only measurements from a single sensor provide incomplete information about the target state, commonly referred to as single-sensor unobservability. In a passive multi-static radar system, the availability of multiple bistatic links naturally lends itself to the fusion of measurements from spatially distributed sensors. However, data fusion emerges as a computationally intensive problem in multi-sensor multi-target tracking algorithms. We propose a two-step sequential approach to solve the underlying problem. We first cast the underlying problem as a group sparse problem in a discretized position-velocity space. A group sparsity based algorithm is applied to simultaneously exploit the multi-static Doppler frequency measurements to directly obtain the instantaneous target state estimates in the Cartesian coordinate system. These estimates are then fed as inputs to the linear Gaussian mixture probability hypothesis density (GMPHD) filter, which removes the false measurements, compensates for missed detections, and reduces the localization error. The optimal sub-pattern assignment metric, which jointly comprises a weighted contribution of cardinality error and localization error, is used to evaluate the performance of the proposed method. Simulation results show that the proposed method successfully handles the multi-target tracking problem and outperforms the existing random receiver selection based multi-sensor implementation of the GMPHD filter.**

***Index Terms*—Passive multi-static radar, multi-target tracking, Doppler-only measurements, group sparsity, GMPHD filter.**

I. Introduction

THE problem of multi-target tracking (MTT) using Doppler-only measurements has emerged as an area of interest, especially in the context of passive multi-static radar (PMR) systems (e.g., [2–5]). This is motivated by the fact that Doppler sensors have become increasingly accurate and inexpensive. A Doppler-only tracking passive radar system comprises an illuminator of opportunity (e.g., DAB/DVB broadcast station, FM radio transmitter, and cellular mobile transmitter), a distributed network of Doppler sensors, and an information fusion center. Alternatively, a network comprising multiple spatially separated transmitters and a single Doppler sensor can be deployed. The former configuration with multiple sensors is more expensive; nonetheless, it is more flexible in configuring a favorable multi-static geometry by placing the sensors at appropriate positions around the available transmitter of opportunity [6]. Doppler-only tracking offers two key advantages in terms of ease-of-implementation and cost, namely, (a) compared to other forms of measurements exploited for high-accuracy tracking in passive radar systems, e.g., time-difference-of-arrival (TDOA) measurements [7], the required accuracy of synchronization among the Doppler sensors is significantly relaxed, and (b) the volume of information exchange, or the bandwidth requirement, for communication among the sensors and/or between each sensor and the information fusion center is significantly reduced. However, from a signal processing perspective, accurate estimation of multi-target states exploiting Doppler frequency measurements subject to additive noise, clutter, and missed detections is a challenging problem. Furthermore, since the Doppler frequency measurement from each sensor provides incomplete information about the target state, commonly known as single-sensor unobservability [8], target state estimation requires a fusion of measurements from multiple spatially distributed sensors. In PMR systems, the availability of multiple bistatic links can be utilized to ensure the required observability through a multi-sensor data fusion, improve overall signal quality, and achieve multi-static diversity gain (e.g., [9–15]). As such, the underlying problem can be concisely cast as a typical multi-sensor MTT problem exploiting Doppler frequency measurements corrupted by additive noise, missed detections, and clutter. The term clutter has been used in the radar signal processing literature in different contexts. In this paper, we refer to clutter as randomly moving objects, other than the actual targets, within the region of surveillance.

Multi-target tracking is a well investigated problem (e.g., [16–19]) relevant to diverse application areas, including air traffic control, intelligence, surveillance, and reconnaissance (ISR), space applications, remote sensing, biomedicine, and

The work of S. Subedi, Y. D. Zhang, and M. G. Amin was supported in part by a subcontract with Defense Engineering Corporation for research sponsored by the Air Force Research Laboratory under Contract FA8650-12-D-1376. Part of the work was presented at the 2015 IEEE International Radar Conference [1].

S. Subedi and M. G. Amin are with the Center for Advanced Communications, Villanova University, Villanova, PA 19085 USA (email: ssubedi1@villanova.edu).

Y. D. Zhang is with the Department of Electrical and Computer Engineering, College of Engineering, Temple University, Philadelphia, PA 19122, USA (email: ydzhang@temple.edu).

B. Himed is with the RF Technology Branch, Air Force Research Laboratory, AFRL/RYMD, Dayton, OH 45433, USA.

robotics. MTT refers to a problem of jointly estimating the number of targets and their states (positions, velocity, etc.), at successive time intervals, from a noisy and cluttered set of observations. The challenges commonly associated with MTT are the time-varying number of targets, false measurements, measurement origin uncertainties, track initiation and management, data association, clutter, and detection loss [17]. There are several algorithms available in the literature that address the problem of multi-target tracking through explicit data association, such as multiple hypothesis tracking (MHT) [18], multi-target particle filter [19], and probabilistic data association (PDA) [20]. These data association based algorithms are combinatorial in nature and suffer from exponentially increasing computational complexity as the number of targets increases. Symmetric measurement equations (SME) [21] and random finite sets (RFS) [22] are two computationally efficient alternatives that avoid explicit data association. The underlying idea of the SME algorithm is to create a 'pseudo-measurement' vector consisting of symmetric functions (e.g., sum of products and sum of powers) of the original measurements, which effectively turns the data association problem into an analytic non-linearity [23]. Such non-linearities are handled using the extended Kalman filter [21] or the unscented Kalman filter [23]. In recent years, the probability hypothesis density (PHD) filter, based on the RFS framework and Bayesian analysis, has gained significant interest in MTT, particularly for problems involving a large number of targets. There are two algorithms available for the implementation of the PHD filter: the sequential Monte Carlo PHD (SMCPHD) [24] and the Gaussian mixture PHD (GMPHD) [25]. The SMCPHD algorithm is more suited to the non-linear target state dynamics, while the GMPHD algorithm provides a closed-form solution and is thus computationally efficient in linear dynamic systems. Multi-Bernoulli filter [26, 27] is another commonly used implementation for RFS based MTT. Unlike the PHD filter, which propagates the first-order moment density, multi-Bernoulli filter propagates the parameters of a multi-Bernoulli distribution that approximates the posterior multi-target density.

Over the years, many approaches have been developed for extending MTT algorithms in a multi-sensor paradigm. Multi-sensor MTT does not lend itself to a simple extension from the single-sensor case owing to the added uncertainties in track formation, track maintenance, and track-to-track association and fusion [28]. The mathematical structure of the optimal solution for multi-sensor MTT has been well analyzed [20, 29]. However, optimal solution to multi-sensor MTT problem using recursive Bayes filter is computationally intractable [30, 31]. As such, multi-sensor MTT remains an open problem from an implementation perspective [32]. It is well established that the explicit data association based algorithms (e.g., MHT, joint probabilistic data association (JPDA) [33]) suffer from a prohibitive computational complexity in a multi-sensor context. In particle filter based algorithms, it becomes necessary to propagate a large number of particles in order to avoid sample impoverishment, rendering these methods practically infeasible [8]. Even for the RFS based algorithms, such as PHD and cardinalized PHD [34], which do not require explicit data associations, their multi-sensor generalization are computationally intractable [35].

The availability of multi-static measurements naturally invites the application of multi-sensor data fusion algorithms in PMR systems. These algorithms, developed in the context of multi-static Doppler-only MTT systems, can be divided into four broad categories [5], namely, centralized measurement fusion, parallel update, sequential update, and random sensor update. It is well known that the centralized measurement fusion mechanism ensures a minimal information loss (e.g., [36–38]) and may possibly achieve an optimal tracking solution. However, despite the obvious advantages in terms of estimation accuracy and robustness, the centralized measurement fusion approach has been exploited only in a very few instances (e.g., [4, 8]), due to the prohibitive associated computational cost. Some of the recent works (e.g., [39, 40]) have proposed computationally efficient techniques to solve the problem of source-measurement association in the PMR systems, which is another critical computational challenge in addition to the target-measurement association. Most of the existing literature in the context of multi-static Doppler-only MTT systems have focused on exploiting sub-optimal approaches such as parallel update, sequential update, or random sensor update to benefit from the availability of multi-static measurements [3, 5, 41]. It is noted that target state estimation in the latter three methods is based on partial information, resulting in a significant information loss. The authors in [5] report the lack of an analytically tractable and computationally acceptable unified multi-sensor fusion method for MTT using Doppler-only measurements. As such, the state of the art for multi-sensor MTT using Doppler-only measurements still lacks a computationally efficient centralized multi-sensor measurement fusion scheme.

In this paper, we propose a novel method for a centralized multi-sensor measurement fusion for MTT using Doppler-only measurements in an PMR system by exploiting the group sparsity shared by the multi-static Doppler frequency measurements in the four-dimensional (4-D) position-velocity space. Specifically, the key contributions of this paper are summarized as follows: (a) We develop a method to transform the scalar Doppler frequency measurements communicated from each sensor to the fusion center to a corresponding time-domain 'pseudo-measurement' in the form of sum of sinusoids. This facilitates the exploitation of the group sparse signal reconstruction in the joint position-velocity domain. It is worth pointing that such a transformation can be applied to several other applications where inexpensive sensors report scalar measurements, such as range-only or bearings-only measurements, to the fusion center rather than the entire raw measurement; (b) We exploit these 'pseudo-measurement' vectors for a centralized multi-sensor fusion method based on group sparse reconstruction in the 4-D discretized position-velocity space. As such, the result of the group sparse reconstruction is obtained directly in the form of the instantaneous multi-target state estimates; and (c) We feed these instantaneous multi-target state estimates as inputs to the GMPHD filter, which handles the missed detections and false measurements, and reduces the overall position estimation error with a low complexity. We evaluate the performance

of the proposed method by comparing the optimal sub-pattern assignment (OSPA) metric [42, 43], which comprises the localization and cardinality errors. Simulation results are provided to validate the capability of the proposed method to successfully handle the multi-target tracking problem in a challenging environment characterized by missed detections and false measurements. Simulation results also show that the proposed method outperforms the random receiver selection based multi-sensor GMPHD filter implementation.

The remainder of the paper is organized as follows. Section II describes the multi-static configuration and develops a Doppler frequency measurement model that assumes missed detections and false measurements. Section III presents a high-level overview of the existing approaches for multi-sensor information fusion for MTT using Doppler-only measurements. Section IV presents the proposed measurement fusion algorithm based on the group-sparsity shared by Doppler frequency measurements at different sensors. Section V presents the RFS based filtering and the GMPHD tracking filter. Section VI analyzes the performance of the proposed method for multi-target state estimation and tracking in terms of the OSPA metric. Section VII provides simulation results and finally conclusions are drawn in Section VIII.

Notations: A lower (upper) case bold letter denotes a vector (matrix). Specifically, $\mathbf{I}_N$ and $\mathbf{0}_N$ denote the $N \times N$ identity and zero matrices, respectively. $(.)^*$, $(.)^T$, and $(.)^H$, respectively, denote complex conjugation, transpose, and hermitian operations. $\mathbb{R}^{n\times 1}$ and $\mathbb{C}^{n\times 1}$, respectively, represent the n-dimensional real and complex vectors. $\|\cdot\|$ denotes the l_2 norm of a vector, whereas $\Re(.)$ and $\Im(.)$, respectively, stand for the real and imaginary parts of a complex number, and $x \sim \mathcal{N}(a, b)$ denotes variable x to be Gaussian distributed with mean a and variance b. We denote $\Pr(.)$ to be the probability density function. In addition, $\mathrm{diag}(.)$ and $\mathrm{tr}(.)$, respectively, denote the diagonal and trace operations.

II. Signal Model

We consider a challenging problem of tracking multiple time-varying ground moving targets in an PMR system characterized by uncertain target detection and false measurements. The PMR network comprises a single broadcast station, transmitting at a known carrier frequency f_c, and N spatially distributed Doppler sensors. The transmitter is assumed to be located at $\mathbf{b}$, whereas the nth receiver is located at $\mathbf{r}^{(n)}$, $n = 1, ..., N$. The transmitter and the Doppler sensors are assumed stationary and their locations are assumed to be precisely known *a priori* at the fusion center.

Let $T(k)$ be the number of targets moving within the surveillance region at the kth observation instant. The number of targets is assumed time-varying, owing to the possible spontaneous appearance/disappearance of targets between two successive measurement instants. The state vector of the ith target at the kth observation, $\mathbf{x}_{k,i}$, represents a point in the state space $\mathbb{X} \in \mathbb{R}^{4\times 1}$ and comprises its instantaneous position $\mathbf{p}_{k,i} \triangleq [p_{x,k,i}, p_{y,k,i}]^T$ and velocity $\mathbf{v}_i \triangleq [v_{x,i}, v_{y,i}]^T$ in the 2-D Cartesian coordinate system, i.e.,

$$\mathbf{x}_{k,i} = [\mathbf{p}_{k,i}^T, \mathbf{v}_i^T]^T. \tag{1}$$

As such, at each observation instant, the ground truth state set is defined as $\mathcal{X}_k \triangleq \{\mathbf{x}_{k,1}, \cdots, \mathbf{x}_{k,T(k)}\}$. The target dynamics is modeled as a linear Gaussian nearly constant velocity model [44], such that

$$\mathbf{x}_{k,i} = \mathbf{F}\mathbf{x}_{k-1,i} + \mathbf{G}\mathbf{w}_{k,i}, \tag{2}$$

for $i = 1, \cdots, T(k)$, where $\mathbf{F}$ is the state transition matrix defined as

$$\mathbf{F} = \begin{bmatrix} \mathbf{I}_2 & \Delta\mathbf{I}_2 \\ \mathbf{0}_2 & \mathbf{I}_2 \end{bmatrix}, \tag{3}$$

where Δ is the sampling interval, and $\mathbf{w}_{k,i} \sim \mathcal{N}(\mathbf{0}, \sigma_{\mathbf{w}}^2\mathbf{I}_2)$ is the process noise modeled as additive white Gaussian noise. The state transition matrix $\mathbf{F}$ represents the linear dynamics, whereas the transition matrix

$$\mathbf{G} = \begin{bmatrix} \frac{\Delta^2}{2}\mathbf{I}_2 \\ \Delta\mathbf{I}_2 \end{bmatrix} \tag{4}$$

accounts for the small acceleration that could deviate the target trajectory from being strictly linear. As such, the process noise covariance matrix is defined as

$$\mathbf{Q} = \sigma_{\mathbf{w}}^2 \begin{bmatrix} \frac{\Delta^4}{4}\mathbf{I}_2 & \frac{\Delta^3}{2}\mathbf{I}_2 \\ \frac{\Delta^3}{2}\mathbf{I}_2 & \Delta^2\mathbf{I}_2 \end{bmatrix}. \tag{5}$$

It is important to acknowledge that this model does not represent a highly maneuvering target.

The actual bistatic Doppler frequency at the nth sensor due to the motion of the ith target is obtained as [11]

$$\breve{f}_{k,i}^{(n)} = -\frac{\mathbf{v}_i^T}{\lambda}\left[\frac{\mathbf{p}_{k,i} - \mathbf{r}^{(n)}}{\|\mathbf{p}_{k,i} - \mathbf{r}^{(n)}\|} + \frac{\mathbf{p}_{k,i} - \mathbf{b}}{\|\mathbf{p}_{k,i} - \mathbf{b}\|}\right], \tag{6}$$

where $\lambda = c/f_c$ is the wavelength of the transmitted signal, and c is the velocity of propagation of a radio signal in the free space. In practice, the Doppler frequency measurements are subject to additive noise, missed detection and measurement uncertainties, such that the bistatic Doppler frequency corresponding to the target state $\mathbf{x}_{k,i}$ measured at the nth sensor is modeled as

$$f_{k,i}^{(n)} = \begin{cases} \breve{f}_{k,i}^{(n)} + \epsilon_{k,i}^{(n)}, & \text{if } \rho_{k,i}^{(n)} = 1, \\ \emptyset, & \text{if } \rho_{k,i}^{(n)} = 0, \end{cases} \tag{7}$$

where $\rho_{k,i}^{(n)} \in \{0, 1\}$ is a Bernoulli random variable with success probability equal to the probability of target detection p_D and $\epsilon_{k,i}^{(n)} \sim \mathcal{N}(0, \sigma_\epsilon^2)$ represents the additive white Gaussian measurement noise. The symbol $\emptyset$ indicates that no measurement is reported in case of a missed detection. The Doppler measurement space or the field-of-view is defined over an interval $[-f_0, f_0]$ [4], where f_0 denotes the maximum possible Doppler frequency. Let us define a set of actual target-generated measurements at the kth observation instant as $\mathcal{T}_k^{(n)} = \{f_{k,1}^{(n)}, \cdots, f_{k,\tau(k)}^{(n)}\}$, where $\tau(k) \leq T(k)$. Incorporating Doppler frequency measurements due to the random movement of clutter into the model, a set of Doppler frequency measurements at the nth sensor observed at the kth observation interval can be defined as

$$\mathcal{D}_k^{(n)} = \mathcal{T}_k^{(n)} \bigcup \mathcal{K}_k^{(n)}, \tag{8}$$

where $\mathcal{K}_k^{(n)}$ with cardinality $K(k)$ represents the set of Doppler frequency measurements due to clutter at the nth sensor observed at the kth observation instant. The position and velocity of such clutter signals are modeled as uniform random variables within the pre-defined range of position and velocity surveillance. As such, the overall cardinality of the Doppler frequency measurement set $\mathcal{D}_k^{(n)}$ is $D(k) = \tau(k) + K(k)$.

In a multi-sensor network, each sensor measures a different Doppler frequency for the motion of the same target, depending on its bistatic configuration. As such, it is not possible to instantaneously fuse these Doppler frequency measurements across different bistatic links [12–14]. As discussed in Section I, due to the prohibitive computational load, most of the existing approaches settle for sub-optimal methods based on partial information, such as sequential update, random receiver selection, and/or parallel update algorithms for exploiting the multi-static measurements. In the following, we provide a high-level description of these existing algorithms for multi-sensor information fusion for MTT using Doppler only measurements.

III. Existing approaches for multi-sensor Doppler-only information fusion for MTT

Existing approaches for multi-sensor information fusion for MTT using Doppler-only measurements can be broadly classified into four categories, namely, parallel update, sequential update, random receiver selection, and centralized measurement fusion. The schematics of each of these scheme is shown in Fig. 1 and explained briefly in the following.

A. Parallel update [5]

As shown in Fig. 1(a), the parallel update, or the typical track-before-fuse approach, involves local tracking at each sensor such that multi-target state is estimated locally based on the partial information available at each sensor. This is followed by a state fusion or track-to-track fusion algorithm, generally in the form of weighted average, at the fusion center. The notations $\hat{\mathcal{X}}_{k-1}$ and $\hat{\mathcal{X}}_k$, respectively, represent the target state estimates obtained at the $(k-1)$th and the kth observation instants, whereas, $\mathcal{D}_k^{(n)}$ and $\hat{\mathcal{X}}_k^{(n)}$, respectively, denote the Doppler frequency measurement set and the local target estimate at the kth observation instant corresponding to the nth sensor. This scheme suffers because of the single-sensor unobservability of Doppler measurements. The local multi-target state estimations include ghost estimates [5], significantly degrading the overall tracking performance. Also, a high computational complexity associated with the track-to-track fusion is a critical concern in multi-target tracking.

B. Sequential update [8, 41]

The sequential update scheme involves inter-sensor communication, where a succeeding sensor uses its local measurements and some form of *a priori* information obtained from a preceding sensor to generate its own estimation. As shown in Fig. 1(b), the Doppler observation $\mathcal{D}_k^{(n)}$ is used to update the state estimate $\hat{\mathcal{X}}_k^{(n-1)}$ in each tracker and yields improved state estimate $\hat{\mathcal{X}}_k^{(n)}$, where $\hat{\mathcal{X}}_{k-1} = \hat{\mathcal{X}}_k^{(0)}$ and $\hat{\mathcal{X}}_k = \hat{\mathcal{X}}_k^{(n)}$ are, respectively, the system input and output at the kth iteration. The process is continued through all available sensors, thereby, reducing the estimation error in each succession. The performance of this method heavily depends on the choice of succession among the sensors. Nonetheless, this method obtains a better solution than the parallel update scheme in most applications (e.g., [5, 8, 41]).

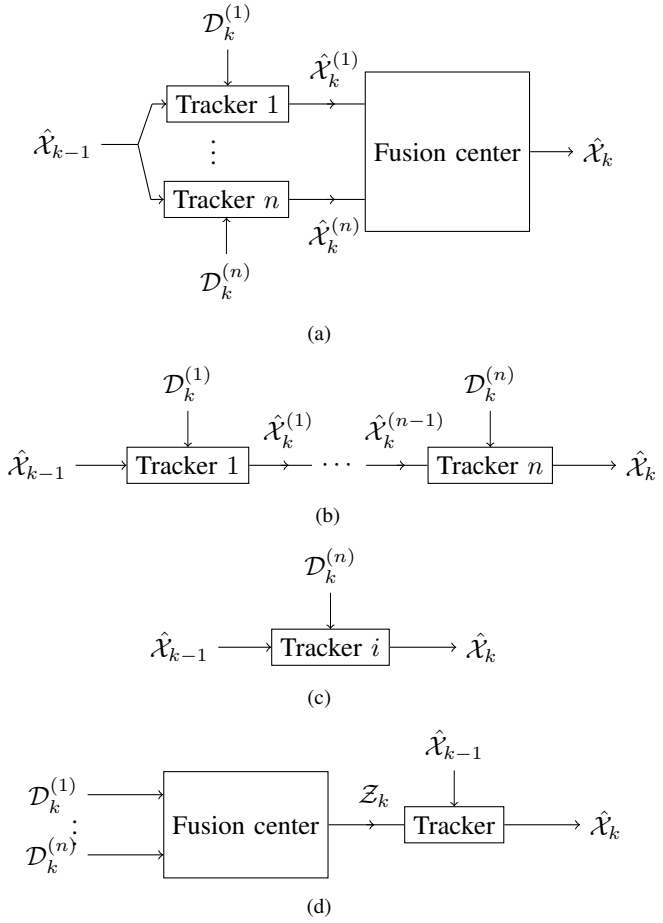

Fig. 1. Existing approaches for multi-sensor fusion in MTT using Doppler-only measurements (a) Parallel update. (b) Sequential update. (c) Random receiver selection. (d) Centralized measurement fusion.

C. Random receiver selection [3]

In the random receiver selection method, illustrated in Fig. 1(c), multi-target target states are estimated at one of the sensors randomly selected at each observation instant [3]. The Doppler observation $\mathcal{D}_k^{(n)}$ is used to update the prior state estimate $\hat{\mathcal{X}}_{k-1}$ at a randomly chosen tracker, in order to obtain the target state estimate $\hat{\mathcal{X}}_k$ at the kth observation. The target state remains unobservable until measurements from at least three spatially distributed sensors are obtained. Furthermore, at each observation instant, a multi-target state set is estimated using the measurement from only one receiver, clearly resulting in a significant loss of information.

D. Centralized measurement fusion [4]

Centralized measurement fusion, or the fuse-before-track, involves a fusion center collecting raw measurements from all the sensors and generating a global multi-target state estimate as shown in Fig. 1(d). The fusion center combines the Doppler frequency measurements at all the sensors, i.e., $\mathcal{D}_k^{(n)}, n = 1, \cdots, N$, and generates a 'super-measurement'

set $\mathcal{Z}_k$, which is fed to the tracking filter as an input. The tracker updates the state estimate $\hat{\mathcal{X}}_k$ exploiting the 'super-measurement' $\mathcal{Z}_k$. Theoretically, this approach exploits all available information and may possibly obtain a globally optimal solution. However, the combinatorial nature of data association in multi-sensor MTT renders this method unrealistic in many practical applications [4].

IV. Multi-sensor measurement fusion exploiting group sparsity

In this section, we propose a computationally tractable method to simultaneously utilize the Doppler frequency measurements available at all sensors by exploiting the group sparsity of the measurements in a discretized position-velocity space. A typical sparse signal reconstruction model is given as

$$\mathbf{g} = \mathbf{A}\boldsymbol{\theta} + \boldsymbol{\eta}, \tag{9}$$

where $\mathbf{g} \in \mathbb{R}^{P\times 1}$ is a measurement vector, $\mathbf{A} \in \mathbb{R}^{P\times Q}$, $P \ll Q$, is a known dictionary matrix, $\boldsymbol{\theta} \in \mathbb{R}^{Q\times 1}$ is the unknown sparse weight vector to be estimated, and $\boldsymbol{\eta} \in \mathbb{R}^{P\times 1}$ is the additive white Gaussian noise vector modeled as $\boldsymbol{\eta} \sim \mathcal{N}(\mathbf{0}, \sigma^2\mathbf{I})$. The fundamental idea behind the sparsity based signal reconstruction is the fact that the measurement vector $\mathbf{g}$ can be represented as a linear combination of K basis vectors in its natural basis or some other sparsifying basis, where $K \ll P$ [45]. In many practical applications, there are multiple measurements arising from a common physical phenomenon. In such cases, for a correctly chosen sparsifying basis, the sparse weight vectors share a common sparse support. Mathematically, such problems are modeled as

$$\mathbf{g}^{(n)} = \mathbf{A}^{(n)}\boldsymbol{\theta}^{(n)} + \boldsymbol{\eta}^{(n)}, \quad n \in [1, \cdots, N], \tag{10}$$

where the sparse weight vectors $\boldsymbol{\theta}^{(n)}$ share the same sparsity support, whereas their values are generally different [46, 47].

In the underlying problem, it is known *a priori* that the targets and clutter are sparsely distributed within the surveillance area for any given observation instant k. As such, the target state space, which represents the position and velocity of the targets, is guaranteed to be sparsely populated. This motivates us to reformulate this problem as a sparse reconstruction problem. Some recent works have proposed the exploitation of the prior knowledge about the sparsity of the signal to improve the tracking performance (e.g., sparsity-aware Kalman tracking [48], hierarchical Bayesian Kalman filters [49], and sparsity-aware multi-target tracking [50, 51]). In addition, we know *a priori* that the Doppler frequency measurements corresponding to N different bistatic pairs are generated due to the same set of targets and clutter moving within the surveillance region. As such, the Doppler frequency measurements share a common sparse support in the discretized position-velocity space inviting the use of group sparse reconstruction for estimating the instantaneous multi-target state.

On the other hand, it is not possible to directly vectorize the Doppler frequency measurement set $\mathcal{D}_k^{(n)}$ at each sensor to form an observation vector compatible to the group sparse reconstruction model in (10). It is important to acknowledge that, in the underlying problem, the sensors communicate only the Doppler frequency measurements instead of the entire raw measurements to the fusion center. This significantly reduces bandwidth requirement and the volume of information exchange between the sensors and the fusion centers. In order to facilitate the group sparsity based measurement fusion, the Doppler frequency measurement set observed at each sensor is represented as a sum of impulses in the discrete Fourier space, which is transformed into the respective time-domain 'pseudo-measurement' through the inverse Fourier transform. As such, each of these time-domain 'pseudo-measurements' becomes a sum-of-sinusoids with frequencies corresponding to the Doppler frequency measurements, which can be used to exploit the group sparsity shared by the multi-sensor Doppler frequency measurements, or equivalently these 'pseudo-measurements', in a discretized position-velocity space.

A. Conversion of the Doppler frequency measurements into time-domain 'pseudo-measurements'

As defined in (8), $\mathcal{D}_k^{(n)}$ with $D(k)$ entries represents the set of Doppler frequency measurements at the nth sensor observed at the kth observation interval corresponding to the $\tau(k)$ target generated measurements and $K(k)$ false measurements. Each of these measurements can be represented as an impulse in a discrete Fourier space and, as such, the entire Doppler spectrum corresponding to the measurement set $\mathcal{D}_k^{(n)}$ can be expressed as a linear sum of impulses in the frequency domain as

$$Y_k^{(n)}(f) = \sum_{i=1}^{D(k)} \delta(f - f_{k,i}^{(n)}), \tag{11}$$

where $f_{k,i}^{(n)} \in [-f_0, f_0]$, as defined in (7). From (11), we obtain the 'pseudo-measurement' in the time-domain as

$$y_k^{(n)}(t) = \sum_{i=1}^{D(k)} \exp(j2\pi f_{k,i}^{(n)} t + \phi_0), \tag{12}$$

where $n = 1, \cdots, N$, $t \in [-\frac{\Delta_y}{2}, \frac{\Delta_y}{2})$ is defined over an observation period Δ_y, and ϕ_0 is an arbitrary initial phase. Sampling the 'pseudo-measurement' observation at a sampling rate F_s yields a total number of $F_s\Delta_y$ samples within the observation period Δ_y. In order to ensure that all the possible Doppler measurements are unambiguously accounted for, the sampling frequency should be chosen to be greater than or equal to the Nyquist rate, i.e., $F_s \geq 2f_0$. The 'pseudo-measurement' observation interval Δ_y should be chosen such that it is consistent with the resolution of the Doppler frequency measurements and also, for a given F_s, satisfies the criteria for the minimum number of observation samples required for sparse signal reconstruction. Without the loss of generality, we set $\phi_0 = 0$. As such, following (7), the discrete time measurements in (12) can be expressed as

$$y_k^{(n)}(t) = \sum_{i=1}^{D(k)} \exp(j2\pi \breve{f}_{k,i}^{(n)} t) \exp(j2\pi \epsilon_{k,i}^{(n)} t). \tag{13}$$

Applying the following Taylor series expansion,

$$\exp(j2\pi\epsilon_{k,i}^{(n)} t) = 1 + \sum_{q=1}^{\infty} \frac{(j2\pi\epsilon_{k,i}^{(n)} t)^q}{q!} \triangleq 1 + \zeta(t),$$

where q is the order of expansion, we obtain

$$y_k^{(n)}(t) = \sum_{i=1}^{D(k)} \exp(j2\pi \breve{f}_{k,i}^{(n)} t) + \xi_{k,i}^{(n)}(t), \tag{14}$$

where $\xi_{k,i}^{(n)}(t) = \zeta(t)\exp(j2\pi \breve{f}_{k,i}^{(n)} t)$ represents the residual additive term in (14). In the underlying problem, for the ith Doppler frequency measurement $f_{k,i}^{(n)}$, since we exploit a single realization of Gaussian random variable $\epsilon_{k,i}^{(n)}$ for all values of t, the distribution of $\xi_{k,i}^{(n)}(t)$ is not strictly Gaussian. Nonetheless, for small values of Doppler frequency measurement errors, $\sigma_\epsilon < 1/(\pi\Delta_y)$, the temporal samples of $\xi_{k,i}^{(n)}(t)$ follow a symmetric distribution centered around zero, which can be closely approximated by a zero-mean Gaussian distribution. The Gaussian approximation becomes closer as the number of Doppler components, $D(k)$, increases. The Gaussianity can be numerically validated using the common statistical normality tests (e.g., the Kolmogorov-Smirnov (KS) test and the Lilliefors test) [52].

In the following, we exploit these time-domain 'pseudo-measurements' to define the observation vectors for group sparse reconstruction.

B. Instantaneous multi-target state estimation using group sparsity

In order to estimate the instantaneous multi-target state by applying group sparsity based signal reconstruction, we represent the entire target state space by a 4-D discrete space comprising $M = M_{px}M_{py}M_{vx}M_{vy}$ points, where M_{px} and M_{py} are the number of points for the position and M_{vx} and M_{vy} are the number of points for the velocity along the x-axis and y-axis, respectively, each point representing a possible target state vector. Since there are limited number of targets and clutter components within the surveillance region, the target state space is sparsely occupied, inviting the exploitation of the sparse reconstruction methods. Let an $M\times 1$ vector $\mathbf{u}_k^{(n)}$ be the unknown sparse vector that vectorizes the discretized 4-D position-velocity space such that each element in $\mathbf{u}_k^{(n)}$ corresponds to a unique possible target state. As such, when a target is represented by the target state vector $\tilde{\mathbf{x}}_{k,\tau} = [\tilde{\mathbf{p}}_{k,\tau}^T, \tilde{\mathbf{v}}_{k,\tau}^T]^T$, where $\tilde{\mathbf{p}}_{k,\tau} = [\tilde{p}_{x,k,\tau}, \tilde{p}_{y,k,\tau}]^T$ and $\tilde{\mathbf{v}}_\tau = [\tilde{v}_{x,\tau}, \tilde{v}_{y,\tau}]^T$, it occupies the τth hypothetical point in the 4-D discrete target state space. In the sparse representation, it corresponds to a non-zero entry at the τth element of $\mathbf{u}_k^{(n)}$. The corresponding bistatic Doppler frequency measurement at the nth sensor can be obtained from (6) as

$$\tilde{f}_{k,\tau}^{(n)} = -\frac{\mathbf{v}_\tau^T}{\lambda}\left[\frac{\tilde{\mathbf{p}}_{k,\tau} - \mathbf{r}^{(n)}}{\|\tilde{\mathbf{p}}_{k,\tau} - \mathbf{r}^{(n)}\|} + \frac{\tilde{\mathbf{p}}_{k,\tau} - \mathbf{b}}{\|\tilde{\mathbf{p}}_{k,\tau} - \mathbf{b}\|}\right], \tag{15}$$

and the corresponding hypothetical 'pseudo-measurement' vector as

$$\tilde{y}_{k,\tau}^{(n)}(t) = \exp(j2\pi \tilde{f}_{k,\tau}^{(n)} t), \tag{16}$$

$t = 1, \cdots, N_s$. Since the multi-static Doppler measurements share a common ground truth in the position-velocity space, the unknown sparse vectors representing the target state space, $\mathbf{u}_k^{(n)}$, can be obtained as the group sparse solution of the following linear formula:

$$\mathbf{y}_k^{(n)} = \mathbf{\Psi}_k^{(n)}\mathbf{u}_k^{(n)} + \boldsymbol{\xi}_k^{(n)}, \quad n = 1, \cdots, N, \tag{17}$$

where $\mathbb{C}^{N_s\times 1}$ vector $\mathbf{y}_k^{(n)} = [y_k^{(n)}(1), \cdots, y_k^{(n)}(N_s)]^T$ represents the observation vector for the kth observation instant, $\mathbf{\Psi}_k^{(n)}$ is the dictionary matrix whose τth column is defined as $\boldsymbol{\psi}_{k,\tau}^{(n)} = [\tilde{y}_{k,\tau}^{(n)}(1), \cdots, \tilde{y}_{k,\tau}^{(n)}(N_s)]^T$, and $\boldsymbol{\xi}_k^{(n)} = [\xi_k^{(n)}(1), \cdots, \xi_k^{(n)}(N_s)]^T$ represents the residual random error vector with elements $\xi_k^{(n)}(t)$ defined in (14). There are a number of algorithms available to solve the group sparse problems such as group basis pursuit [53], group LASSO [54], and block orthogonal matching pursuit [55]. Multi-task Bayesian compressive sensing algorithm [56, 57] provides an adaptive learning framework and generally outperforms the conventional compressive sensing algorithms. In this paper, we use the complex multi-task Bayesian compressive sensing (CMT-BCS) algorithm [57], which is based on the Bayesian framework that exploits the statistical relationship between multiple measurements or sensing tasks and that between the real and imaginary parts of the complex-valued sparse entries. It is noted that the missed detections and/or false alarms at some of the sensors results in a partial common support among the groups. As shown in [56], the multi-task Bayesian compressive sensing algorithm is able to learn the level of sparsity adaptively from such partial common sparse support and effectively solve the group sparse reconstruction problem under the partial common sparse support. Herein, we briefly describe the application of the CMT-BCS algorithm in the context of the underlying problem, whereas the comprehensive analysis of the method is presented in [57].

The CMT-BCS algorithm places a Gaussian distribution on the elements of the sparse vector $\mathbf{u}_k^{(n)} = [u_{1,k}^{(n)}, \cdots, u_{M,k}^{(n)}]^T$ such that the real and imaginary components follow an independent Gaussian distribution with zero mean and variance $\alpha_{\tau,k}$, defined as

$$\begin{aligned} \Re(u_{\tau,k}^{(n)}) &\sim \mathcal{N}(0, \alpha_{\tau,k}), \\ \Im(u_{\tau,k}^{(n)}) &\sim \mathcal{N}(0, \alpha_{\tau,k}), \end{aligned} \tag{18}$$

where $\tau \in [1, \cdots, M]$. The core philosophy behind the CMT-BCS algorithm is that the parameters $\boldsymbol{\alpha}_k = \{\alpha_{\tau,k}\}_{\tau=1,\cdots,M}$ are shared across the N bistatic links and also across the real and imaginary components of the sparse complex coefficients. Likewise, a Gaussian prior approximation is placed on the residual additive error term $\xi_k^{(n)}(t)$, such that

$$\begin{aligned} \Re(\xi_k^{(n)}(t)) &\sim \mathcal{N}(0, \beta_{0,k}), \\ \Im(\xi_k^{(n)}(t)) &\sim \mathcal{N}(0, \beta_{0,k}), \end{aligned} \tag{19}$$

where $t = 1, \cdots, N_s$ and $\beta_{0,k}$ is the error variance. The CMT-BCS exploits the Bayesian inference to evaluate the posterior density function for the sparse vector $\bar{\mathbf{u}}_k^{(n)} = [\Re(\mathbf{u}_k^{(n)})^T, \Im(\mathbf{u}_k^{(n)})^T]^T$, such that

$$\Pr(\bar{\mathbf{u}}_k^{(n)} | \bar{\mathbf{y}}_k^{(n)}, \mathbf{\Psi}_k^{(n)}, \boldsymbol{\alpha}_k, \beta_{0,k}) = \mathcal{N}(\boldsymbol{\mu}_k^{(n)}, \mathbf{\Sigma}_k^{(n)}), \tag{20}$$

where

$$\boldsymbol{\mu}_k^{(n)} = \beta_{0,k}^{-1}\mathbf{\Sigma}^{(n)}\bar{\mathbf{\Psi}}_k^{(n)T}\bar{\mathbf{y}}_k^{(n)}, \tag{21}$$

$$\boldsymbol{\Sigma}_k^{(n)} = \left[\beta_{0,k}^{-1}\bar{\boldsymbol{\Psi}}_k^{(n)T}\bar{\boldsymbol{\Psi}}_k^{(n)} + \mathbf{A}^{-1}\right]^{-1}, \tag{22}$$

$$\bar{\boldsymbol{\Psi}}_k^{(n)} = \begin{bmatrix} \Re(\boldsymbol{\Psi}_k^{(n)}) & -\Im(\boldsymbol{\Psi}_k^{(n)}) \\ \Im(\boldsymbol{\Psi}_k^{(n)}) & \Re(\boldsymbol{\Psi}_k^{(n)}) \end{bmatrix}, \tag{23}$$

$$\mathbf{A}_k = \operatorname{diag}\left(\left[\alpha_{1,k}, \cdots, \alpha_{M,k}, \alpha_{1,k}, \cdots, \alpha_{M,k}\right]^T\right), \tag{24}$$

and $\bar{\mathbf{y}}_k^{(n)} = [\Re(\mathbf{y}_k^{(n)})^T, \Im(\mathbf{y}_k^{(n)})^T]^T$. The expectation maximization (EM) estimate for the $\alpha_{\tau,k}$ and $\beta_{0,k}$ are given as [57]

$$\alpha_{\tau,k} = \frac{1}{N}\sum_{n=1}^{N}\left(\mu_{k,\tau}^{(n)2} + \mu_{k,M+\tau}^{(n)2} + \Sigma_{k,\tau\tau}^{(n)} + \Sigma_{k,(M+\tau)(M+\tau)}^{(n)}\right), \tag{25}$$

where $\mu_{k,\tau}^{(n)}$ and $\Sigma_{k,\tau\tau}^{(n)}$, respectively, represent the τth element of the mean vector $\boldsymbol{\mu}_k^{(n)}$ and τth diagonal element of the covariance matrix $\boldsymbol{\Sigma}_k^{(n)}$, where as

$$\beta_{0,k} = \frac{1}{2MN}\left\{\sum_{n=1}^{N}\operatorname{tr}\left(\boldsymbol{\Sigma}_k^{(n)}\bar{\boldsymbol{\Psi}}_k^{(n)}\bar{\boldsymbol{\Psi}}_k^{(n)T}\right) + \|\bar{\mathbf{y}}_k^{(n)} - \bar{\boldsymbol{\Psi}}_k^{(n)}\boldsymbol{\mu}_k^{(n)}\|^2\right\}. \tag{26}$$

As such, from (21) and (22), we can respectively obtain the mean and the variance of the elements of the sparse vector $\mathbf{u}_k^{(n)}$ once we know the parameters $\boldsymbol{\alpha}_k$ and $\beta_{0,k}$, and these parameters are recursively updated using equations (21), (22), (25), and (26) until a convergence criterion is satisfied. Thus, the CMT-BCS algorithm effectively exploits the group sparsity between the real and the imaginary parts of the sparse entries, $\Re(\mathbf{u}_k^{(n)})$ and $\Im(\mathbf{u}_k^{(n)})$, and for every observation interval k, the solution $\mathbf{u}_k^{(n)} = \Re(\mathbf{u}_k^{(n)}) + j\Im(\mathbf{u}_k^{(n)})$ converges to a $\hat{T}(k)$-sparse solution. The index of each element in the support of the estimated sparse vector corresponds to a point in the discrete target state space. As such, the $\hat{T}(k)$-sparse solution corresponds to $\hat{T}(k)$ instantaneous target state estimates, $\mathbf{z}_{k,i} = [\hat{p}_{x,k,i}, \hat{p}_{y,k,i}, \hat{v}_{x,k,i}, \hat{v}_{y,k,i}]^T$, where $i = 1, \cdots, \hat{T}(k)$. Also, since the CMT-BCS algorithm is known to be less sensitive to the dictionary coherence, it is a good choice for the underlying problem where it is desirable to have a high resolution measurement matrix. As such, at every k, we obtain instantaneous multi-target state estimates, i.e.,

$$\mathcal{Z}_k = \{\mathbf{z}_{k,1}, \cdots, \mathbf{z}_{k,\hat{T}(k)}\}. \tag{27}$$

Once we obtain the instantaneous target state estimates by fusing the multi-sensor Doppler-only measurements through the exploitation of group sparse reconstruction based centralized multi-sensor measurement fusion, there are three specific tasks remaining from a tracking perspective: (a) improving the cardinality estimation by removing the clutter and the false estimates that occur in the group sparse reconstruction, and compensating for the missed detection, and (b) improving the localization accuracy by gradually learning from the instantaneous target state estimates $\mathcal{Z}_k$ and the pre-defined target dynamic model. As discussed in Section I, through the group sparsity based centralized measurement fusion scheme, we effectively transform the multi-sensor MTT problem, exploiting non-linear Doppler-only measurements, into a single-sensor MTT problem using linear measurements in the form of target-state estimates. This allows us to apply the computationally efficient linear Kalman filter based GMPHD filter to handle the aforementioned two specific tracking tasks.

C. Compliance to the assumptions of the GMPHD filter

The PHD filter is a principled solution developed on the foundation of RFS approach to MTT, which is valid under the following specific assumptions [22, 25, 26].

A.1 Each target evolves and generates observations independent of one another.

A.2 Clutter is Poisson distributed and independent of target-originated measurements.

These two assumptions are common to all variants of the PHD filter. The Gaussian mixture implementation of the PHD filter requires the following three additional assumptions to hold [25].

A.3 Each target follows a linear Gaussian dynamical model and the measurement model is also linear Gaussian.

A.4 The survival and detection probabilities are state independent.

A.5 The intensities of the birth RFSs can be represented as Gaussian mixtures.

In this paper, as we implement the GMPHD filter for MTT exploiting the output from the CMT-BCS algorithm as the measurements to the GMPHD filter, herein we present a pointwise analysis of the compliance of the statistical characteristics of these measurements to the aforementioned assumptions.

C.1 In order to apply the group sparse reconstruction algorithm, we discretize the entire 4-D target state space such that each element of the sparse vector represents a unique point in the target space. The dictionary matrix is constructed such that its columns are linearly independent. As such, the unique representation property condition is satisfied to guarantee the sparse signal recovery with a high probability [57]. Therefore, for each target, the CMT-BCS generates an instantaneous target state estimate (referred to as observations in A.1.), independent of other targets.

C.2 The signal model inherently embeds the fact that each target evolves independently.

C.3 As discussed earlier, the output of the CMT-BCS algorithm comprises estimates corresponding to three different classes of objects/events; (a) true targets; (b) clutter described as the randomly moving objects, other than the actual targets, within the region of surveillance; and (c) a small number of spurious estimates that may occur occasionally during the group sparse reconstruction due to the additive noise as defined in (17). Since the clutter is assumed to be Poisson distributed and the spurious estimates occur in small numbers and occasionally, it is justified to approximately group these two classes of objects/events together as a Poisson distributed variable with a mean value equal to the number of clutters. Also, it is important to note that all these objects/events generate outputs in the CMT-BCS algorithm independently of one another.

C.4 The dynamics of each target is assumed to be linear Gaussian as defined in (2), and the corresponding measurement model is also Gaussian as the CMT-BCS algorithm places

a Gaussian distribution on the elements of the sparse vector as discussed in (18).

C.5 The assumption that the survival and detection probabilities are state independent is inherent to the signal model.

C.6 The intensities of the birth RFSs are represented as Gaussian mixtures.

V. Gaussian mixture PHD filter

In this section, we apply the GMPHD filter proposed in [25] to solve the underlying problem. The GMPHD filter provides a closed-form solution to the computationally efficient multi-target PHD filter under linear Gaussian multi-target models. It is noted that, unlike the existing works (e.g., [3, 4]) that require an EKF based adaptation of the GMPHD filter in order to handle non-linear Doppler frequency measurements, we can implement linear Gaussian multi-target models discussed in [25], since the output of the CMT-BCS algorithm is directly obtained in the form of target state estimates. Also, this avoids the need to adopt other non-linear filtering approaches for RFS filtering such as SMCPHD or particle filter implementation, which are commonly used in tracking problems using Doppler-only measurements (e.g. [4, 5, 8]). The details of the GMPHD filter implementation for the underlying problem is as follows.

An RFS model for the time evolution of a multi-target state $\mathcal{X}_k$ at time k from $\mathcal{X}_{k-1}$ is defined as

$$\mathcal{X}_k = \left[\bigcup_{\boldsymbol{\zeta}\in\mathcal{X}_{k-1}} \mathcal{S}_{k|k-1}(\boldsymbol{\zeta})\right] \bigcup \Gamma_k, \tag{28}$$

where $\mathcal{S}_{k|k-1}(\boldsymbol{\zeta})$ represents the RFS of the surviving targets from the preceding state $\boldsymbol{\zeta}$, and Γ_k is the RFS of the spontaneous target births at time k. The corresponding RFS measurement model observed at the kth observation can be expressed as

$$\mathcal{Z}_k = \Upsilon_k \bigcup \left[\bigcup_{\mathbf{x}\in\mathcal{X}_k} \Theta_k(\mathbf{x})\right], \tag{29}$$

where Υ_k is the RFS of the clutter measurements and the false estimates that occur during the group sparse reconstruction, and $\Theta_k(\mathbf{x})$ is the RFS of the actual target-generated measurements.

The GMPHD filter propagates the Gaussian mixture posterior intensity in time to significantly reduce the computational complexity in the multi-target Bayes filter. The latter is a consequence of the combinatorial nature of the multi-target densities and multiple integrations on the multi-target state space [25]. It is assumed that the posterior intensity at time $k-1$ can be written as a sum of J_{k-1} Gaussian components with different weights $w_{k-1}^{(i)}$, mean vectors $\mathbf{m}_{k-1}^{(i)}$ and covariance matrices $\mathbf{P}_{k-1}^{(i)}$ as

$$\nu_{k-1}(\mathbf{x}) = \sum_{i=1}^{J_{k-1}} w_{k-1}^{(i)} \mathcal{N}(\mathbf{x}; \mathbf{m}_{k-1}^{(i)}, \mathbf{P}_{k-1}^{(i)}), \tag{30}$$

where the Gaussian mixture $\{(w_{k-1}^{(i)}, \mathbf{m}_{k-1}^{(i)}, \mathbf{P}_{k-1}^{(i)})\}_{i=1}^{J_{k-1}}$ is a union of two Gaussian mixture components corresponding to the persistent target and new born targets.

Likewise, the predicted intensity can also be formulated as a sum of the predicted intensities of the persistent and the new born targets, such that

$$\nu_{k|k-1}(\mathbf{x}) = \nu_{k|k-1,\mathrm{p}}(\mathbf{x}) + \gamma_k(\mathbf{x}), \tag{31}$$

where the predicted intensity of the persistent targets is assumed to be a Gaussian mixture and is defined as

$$\nu_{k|k-1,\mathrm{p}}(\mathbf{x}) = \sum_{i=1}^{J_{k-1,p}} w_{k|k-1,\mathrm{p}}^{(i)} \mathcal{N}(\mathbf{x}; \mathbf{m}_{k|k-1,\mathrm{p}}^{(i)}, \mathbf{P}_{k|k-1,\mathrm{p}}^{(i)}), \tag{32}$$

where $w_{k|k-1,\mathrm{p}}^{(i)} = p_s w_{k-1}^{(i)}$, $\mathbf{m}_{k|k-1,\mathrm{p}}^{(i)} = \mathbf{F}\mathbf{m}_{k-1}^{(i)}$, and $\mathbf{P}_{k|k-1,\mathrm{p}}^{(i)} = \mathbf{Q} + \mathbf{F}\mathbf{P}_{k-1}^{(i)}\mathbf{F}^T$. Likewise, the intensity of the new born targets is also assumed to be a Gaussian mixture defined as

$$\gamma_k(\mathbf{x}) = \sum_{i=1}^{J_{k,\mathrm{b}}} w_{k,\mathrm{b}}^{(i)} \mathcal{N}(\mathbf{x}; \mathbf{m}_{k,\mathrm{b}}^{(i)}, \mathbf{P}_{k,\mathrm{b}}^{(i)}), \tag{33}$$

where $w_{k,\mathrm{b}}^{(i)}$, $\mathbf{m}_{k,\mathrm{b}}^{(i)}$, and $\mathbf{P}_{k,\mathrm{b}}^{(i)}$, respectively, represent the weight, mean vector and covariance matrix of the birth intensity.

The standard formulation of the PHD filter assumes that the target birth intensity is known a priori [24, 25, 58]. Typically, the birth components are defined as intensities whose mass is concentrated over small specific areas or hotspots in the state space. In the event when a target appears in a region that is not covered by the predefined birth intensity, the PHD filter will be completely blind to its existence. In order to avoid such situation, the generally adopted approach is to define rather diffused birth intensities such that they cover the entire state space of interest. However, that results in a higher incidence of short-lived false tracks and longer confirmation times [58]. In that context, instead of randomly initializing diffused target birth intensities [3], we use the instantaneous target state estimates obtained from the CMT-BCS algorithm at each observation instant to initialize the target birth intensities. The corresponding values of the non-zero elements are used as the weights of the Gaussian components. It is important to note that we initialize the birth components in the vicinity of the instantaneous target state estimates obtained from the CMT-BCS algorithm, but with much larger variances and weights that are equal to the corresponding non-zero elements in the estimated sparse vector. This creates a few large hotspots within the target state space with different weights. In this respect, it is different from the vanilla measurement-driven birth component described in [58], where in the SMC implementation of the PHD/CPHD filters, the authors model the birth intensity by an equally weighted mixture of birth densities. The latter comprise particles drawn directly from the measured subspace of the target state space. The authors introduce an additional variable to distinguish between the persistent target and a new-born target, and accordingly deploy a modified prediction and update procedure to correct the bias due to measurement-driven initialization.

Following the preceding analysis, the posterior intensity for time k is also a Gaussian mixture given as

$$\nu_k(\mathbf{x}) = (1-p_D)\nu_{k|k-1}(\mathbf{x}) + \sum_{\mathbf{z}\in Z_k}\sum_{i=1}^{J_{k|k-1}} w_k^{(i)}(\mathbf{z})\mathcal{N}(\mathbf{x};\mathbf{m}_{k|k}^{(i)}(\mathbf{z}),\mathbf{P}_{k|k}^{(i)}), \tag{34}$$

where

$$w_k^{(i)}(\mathbf{z}) = \frac{p_D w_{k|k-1}^{(i)} q_k^{(i)}(\mathbf{z})}{\upsilon_k(\mathbf{z}) + p_D \sum_{j=1}^{J_{k|k-1}} w_{k|k-1}^{(j)} q_k^{(j)}(\mathbf{z})}, \tag{35}$$

$$q_k^{(i)}(\mathbf{z}) = \mathcal{N}(\mathbf{z};\mathbf{H}_k\mathbf{m}_{k|k-1}^{(i)}, \mathbf{R}_k + \mathbf{H}_k\mathbf{P}_{k|k-1}^{(i)}\mathbf{H}_k^T), \tag{36}$$

$$\mathbf{m}_{k|k}^{(i)}(\mathbf{z}) = \mathbf{m}_{k|k-1}^{(i)} + \mathbf{K}_k^{(i)}(\mathbf{z} - \mathbf{H}_k\mathbf{m}_{k|k-1}^{(i)}), \tag{37}$$

$$\mathbf{P}_{k|k}^{(i)} = \left[\mathbf{I} - \mathbf{K}_k^{(i)}\mathbf{H}_k\right]\mathbf{P}_{k|k-1}^{(i)}, \tag{38}$$

$$\mathbf{K}_k^{(i)} = \mathbf{P}_{k|k-1}^{(i)}\mathbf{H}_k^T(\mathbf{H}_k\mathbf{P}_{k|k-1}^{(i)}\mathbf{H}_k^T + \mathbf{R}_k)^{-1}, \tag{39}$$

where $\upsilon_k(\mathbf{z})$ is the intensity of the RFS Υ_k which represents the clutter measurements and the false estimates that occur during the group sparse reconstruction at time k. Since the group sparsity based measurement fusion yields the target state estimates, which are directly fed as instantaneous observations to the GMPHD filter, the observation matrix is a 4×4 identity matrix, such that $\mathbf{H}_k = \mathbf{I}_4$, and the $\mathbf{R}_k$ is the observation noise covariance matrix.

From an implementation perspective, the computational load increases with the increasing number of Gaussian components with time. It is analytically shown in [25] that the number of components in the posterior intensities increases without any bound. As such, pruning and merging are commonly adopted to ensure a limit on the number of Gaussian components propagated in each succession. Pruning refers to a process of propagating a fixed number of targets with the strongest weights in each succession or discarding the targets that have weights below some pre-determined threshold. Merging, on the other hand, involves approximating closely-located multiple Gaussian components by a single Gaussian. The process of pruning and merging is explained in detail in [25]. Once the posterior intensity is computed, followed by pruning and merging, the multi-target state estimates $\tilde{\mathcal{X}}_k = \{\tilde{\mathbf{x}}_{k,1}, \cdots, \tilde{\mathbf{x}}_{k,\tilde{T}(k)}\}$ is extracted by selecting the means of the Gaussian components that have weights greater than some threshold.

The schematics in Fig. 2 summarizes the proposed algorithm comprising the following three key steps: (a) conversion of a set of scalar Doppler observations $\mathcal{D}_k^{(n)}$ into time-domain 'pseudo-measurement' vectors $\mathbf{y}_k^{(n)}$ corresponding to each of the N bistatic links, (b) application of the CMT-BCS algorithm to fuse the multi-sensor information by exploiting the group sparsity shared by the Doppler measurements in the discretized position-velocity space to obtain the sparse solution that converges to a single set of instantaneous target state estimates $\mathcal{Z}_k$ that represents all the bistatic links, and (c) application of GMPHD filtering to remove the false

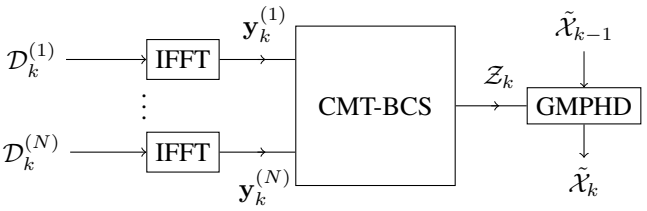

Fig. 2. Schematics of the proposed algorithm.

measurements, compensate for missed detections, and reduce the localization error from $\mathcal{Z}_k$, leading to an improved target state estimate set $\tilde{\mathcal{X}}_k$.

It is noteworthy that, with the increase in the cardinality of the Doppler measurement set and/or the number of sensors, the increment in the computational cost associated with the proposed method for multi-sensor information fusion is significantly lower compared to the optimal centralized measurement fusion process. Specifically, the computational cost associated with the optimal centralized measurement fusion for multi-sensor multi-target tracking algorithm is combinatorial, i.e., for the underlying problem, with N Doppler sensors and $D(k)$ Doppler measurements per sensor at the kth observation, the computational complexity of the optimal centralized measurement fusion is of the order $\mathcal{O}((D(k)!)^N)$ [59]. On the other hand, the computational cost associated with the proposed method for centralized measurement which exploits the group sparse reconstruction in the position-velocity domain is of the order $\mathcal{O}(D(k)N_sMN)$ [60], where N_s is the number of samples in the pseudo-measurement vectors $\mathbf{y}_k^{(n)}$, and M is the number of discrete points each representing a possible target state in the discretized target state space. As such, the proposed method is better poised to handle a situation with a larger number of sensors and/or larger number of Doppler measurements per sensor.

In the following, we analyze the performance of the proposed method in terms of the OSPA error in the estimation of the instantaneous multi-target state using group sparse reconstruction and after the application of the tracking filter.

VI. Performance analysis

The performance of multi-target estimation and tracking algorithms is commonly evaluated in terms of the OSPA metric (e.g. [42], [43]). The OSPA metric jointly evaluates the performance of the estimation algorithm as a weighted contribution of both cardinality error and localization error. We calculate the OSPA metric at the end of each step to isolate the causes of error and also to demonstrate the improvement in performance after the application of the GMPHD filter.

It is noted that, since the actual number of targets at each observation instant is unknown *a priori*, we use a relaxed sparsity constraint in the CMT-BCS algorithm to ensure that all detected targets, including the weak ones, are accounted for. As such, due to the use of such relaxed sparsity constraint in addition to the presence of clutter measurements, the cardinality of the estimated target state set $\mathcal{Z}_k$ is generally larger than the cardinality of the ground truth state $\mathcal{X}_k$, i.e., $\hat{T}(k) \geq T(k)$, resulting in a cardinality error. On the other

hand, due to the Doppler frequency measurement error, the target state estimates may deviate from the ground truth state, causing the localization error. The cardinality error between the ground truth state and estimated instantaneous target state at the kth observation instant is given by

$$e_{p,c}^{\text{card}}(k) = \left[\frac{(\hat{T}(k) - T(k))c^p}{\hat{T}(k)}\right]^{\frac{1}{p}}, \tag{40}$$

where $1 \leq p < \infty$ is the order of the OSPA distance, and $c > 0$ represents the cut-off parameter. Similarly, the localization error is defined as

$$e_{p,c}^{\text{loc}}(k) = \left[\frac{1}{\hat{T}(k)} \cdot \min_{\pi \in \Pi_{\hat{T}(k)}} \sum_{i=1}^{T(k)} (d_c(\mathbf{x}_{k,i}, \mathbf{z}_{\pi,k,i}))^p\right]^{\frac{1}{p}}, \tag{41}$$

where $\Pi_{\hat{T}(k)}$ represents the set of permutations of length $T(k)$ with elements taken from $\{1, 2, \cdots, \hat{T}(k)\}$, and $d_c(\mathbf{x}_{k,i}, \mathbf{z}_{\pi,k,i}) = \min(c, d(\mathbf{x}_{k,i}, \mathbf{z}_{\pi,k,i}))$, with $d(\mathbf{x}_{k,i}, \mathbf{z}_{\pi,k,i})$ being the base distance between the two tracks at k. The cut-off parameter c is used to assign a relative weight to the cardinality error against the localization error. A higher value of c corresponds to a higher weight assigned to the cardinality error and vice versa. The order parameter, p, determines the penalty assigned for the 'outlier' estimates that significantly deviate from any of the ground truth tracks. A higher p results in a higher sensitivity to such outliers. For cases where $\hat{T}(k) < T(k)$, however rare, the cardinality error and localization error are, respectively, defined as $e_{p,c}^{\text{card}}(k)(\mathcal{X}_k, \mathcal{Z}_k) = e_{p,c}^{\text{card}}(k)(\mathcal{Z}_k, \mathcal{X}_k)$ and $e_{p,c}^{\text{loc}}(k)(\mathcal{X}_k, \mathcal{Z}_k) = e_{p,c}^{\text{loc}}(k)(\mathcal{Z}_k, \mathcal{X}_k)$. As such, the overall OSPA error in multi-target state estimation, comprising cardinality and localization error, is calculated as

$$e_{p,c}^{\text{GS}}(k) = \left[\frac{1}{\hat{T}(k)} \cdot \min_{\pi \in \Pi_{\hat{T}(k)}} \sum_{i=1}^{T(k)} (d_c(\mathbf{x}_{k,i}, \mathbf{z}_{\pi,k,i}))^p + \frac{(\hat{T}(k) - T(k))c^p}{\hat{T}(k)}\right]^{\frac{1}{p}}. \tag{42}$$

The GMPHD filter removes the clutter and the false estimates that occur during the group sparse reconstruction and compensates for the missed detections resulting in a significant reduction in the cardinality error. Also, the tracking filter reduces the localization error by intelligently learning from the instantaneous target state estimates and the pre-defined target dynamics. As such, following (40)–(42) and the associated definitions, the overall OSPA error between the ground truth multi-target state $\mathcal{X}_k$ and the estimated multi-target state $\tilde{\mathcal{X}}_k$ is defined as

$$\tilde{e}_{p,c}^{\text{GMPHD}}(k) = \left[\frac{1}{\tilde{T}(k)} \cdot \min_{\pi \in \Pi_{\tilde{T}(k)}} \sum_{i=1}^{T(k)} (d_c(\mathbf{x}_{k,i}, \tilde{\mathbf{x}}_{\pi,k,i}))^p + \frac{(\tilde{T}(k) - T(k))c^p}{\tilde{T}(k)}\right]^{\frac{1}{p}}. \tag{43}$$

In the following, we present numerical examples to validate the performance of the proposed method for different target trajectories and to compare the performance of the proposed method against the existing random receiver selection based multi-sensor implementation of the GMPHD filter for MTT using Doppler-only measurements.

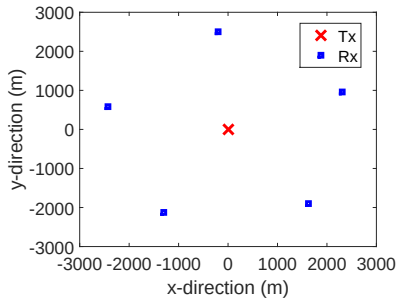

Fig. 3. Passive multi-static radar network configuration using multiple Doppler sensors.

VII. Simulation Results

In the simulations, we consider a PMR network configuration as illustrated in Fig. 3, where a broadcast station is located at the origin and transmitting at 950 MHz, and 5 Doppler frequency measurement sensors are distributed along a circle of radius 2.5 km from the transmitter. The transmitter and the sensors are assumed stationary and their positions precisely known *a priori* at the fusion center. The region of surveillance is assumed to be a rectangular area bounded by $[-2500, 2500]^T$ m along both the x- and y-axes.

We consider four simulation examples with different multi-target trajectories to test the performance of the proposed method in different complexities: (a) non-crossing trajectories with linear constant velocity, (b) intersecting trajectories with linear constant velocity, (c) trajectories with nearly-constant velocity, (d) and time-varying number of targets.

We use the simulation parameters shown in Table I for all four cases. The false measurement is modeled as a

TABLE I
Simulation Parameters.

Parameter	**Value**
Sampling interval (Δ)	0.5 s
Observation period of the 'pseudo-measurement' (Δ_y)	1 s
Maximum possible Doppler frequency measurement (f_0)	250 Hz
Sampling rate of the 'pseudo-measurement'(F_s)	512 Hz
Standard deviation of process noise (σ_w)	1 m/s^2
Frequency of operation	950 MHz
Standard deviation of measurement noise (σ_ϵ)	0.3 Hz
Probability of target detection (p_D)	0.98
Probability of target survival (p_S)	0.99

Poisson RFS with an average number of 5 false measurements generated due to the random movement of different objects other than the actual targets within the region of surveillance. For pruning, we consider the truncation level to be 10^{-5} and the maximum number of Gaussian components is considered to be $J_{\max} = 50$. Likewise, we merge the Gaussian components with Mahalanobis distance of less than 4. We use the birth covariance matrix $\mathbf{P}_{k,\text{b}}^{(i)} = \text{diag}([400, 400, 100, 100]^{\text{T}})$ and the observation noise covariance matrix $\mathbf{R}_k = \text{diag}([100, 100, 25, 25]^{\text{T}})$. For calculating the OSPA error metric, we consider the cut-off parameter

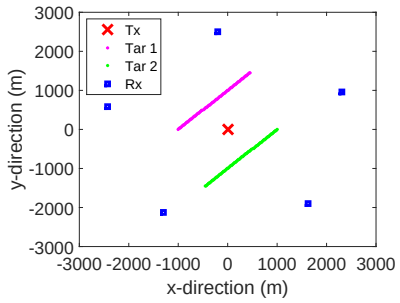

Fig. 4. Non-crossing target trajectories with linear constant velocity.

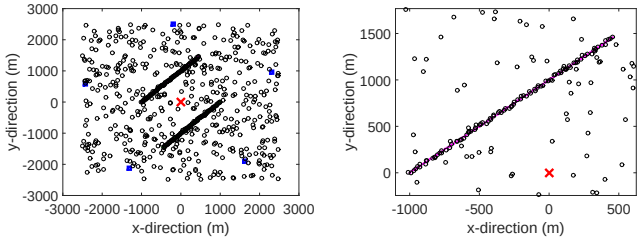

Fig. 5. Instantaneous target state estimation using group sparse reconstruction (a) Entire surveillance area. (b) Enlarged view around the trajectory of the first target.

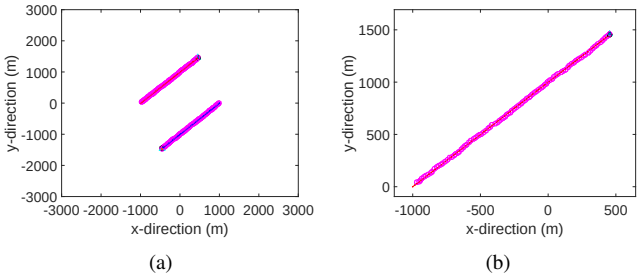

Fig. 6. Results of the GMPHD filter. (a) Entire surveillance area. (b) Enlarged view around the trajectory of the first target.

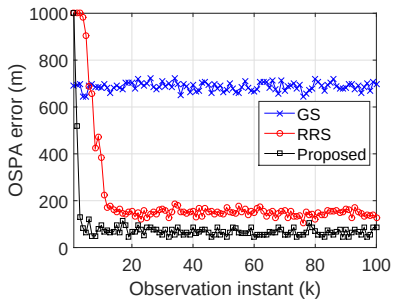

Fig. 7. Performance of the proposed method and the random receiver selection based method for non-crossing target trajectories with linear constant velocity.

$c = 1000$ and order of the OSPA distance $p = 1$. Note that for a sampling frequency of 512 Hz and an observation interval of 1 s, we obtain a sufficient number of samples of 'pseudo-measurements' for sparse signal reconstruction. Also, for an observation interval of 1 s and standard deviation of the Doppler frequency measurement noise equal to 0.3 Hz, the residual additive term in (14) can be approximated as a Gaussian random variable. We verified this using the KS normality test at 2% level of significance.

A. Non-crossing target trajectories with linear constant velocity

We consider two targets initially located at $[-1000, 0]^T$ m and $[1000, 0]^T$ m and travelling along linear trajectories with velocities $[30, 30]^T$ m/s and $[-30, -30]^T$ m/s, respectively, as shown in Fig. 4. The corresponding target state estimates obtained using the group sparsity based approach are shown in Fig. 5. We observe that, by exploiting the group sparsity of the multi-static Doppler frequency measurements in the discretized position-velocity space, the CMT-BCS algorithm yields the estimated target positions closely grouped around the actual target trajectories throughout the observation period. However, the instantaneous target state estimation algorithm based on group sparse reconstruction cannot discern between the true target generated measurements and the clutter generated measurements. Also, since the number of targets is unknown, a safe threshold is chosen to relax the sparsity constraint in the CMT-BCS algorithm. As a result, we observe false measurements distributed over the observation scene. Also, we notice uncertain target detection artifacts in the form of some missing points along the target trajectories. The estimated trajectories of the targets after GMPHD filtering are shown in Fig. 6. It is evident that, at the steady state, the tracking filter reduces the overall cardinality and localization errors by removing the false measurements, compensating for the missed detections, and smoothing the true target state estimates.

The performance of the proposed method in terms of the OSPA metric for multi-target tracking is shown in Fig. 7. We can observe that the overall OSPA error remains close to 725 m due to a dominant cardinality error in multitarget state estimation using the CMT-BCS algorithm. As discussed earlier, this is because the group sparse reconstruction based instantaneous target estimation technique cannot discern between the false measurements and the true targets and a relaxed sparsity constraint is used to ensure that the weaker targets are also accounted for. Also, it cannot compensate for the missed detections. On the other hand, the overall OSPA error is significantly reduced after GMPHD filtering, as the tracking filter successfully removes the false measurements, compensates for the missed detection, and successively reduces the localization error. On the other hand, the random receiver selection based approach initially takes more observations to converge to the error floor and, even upon convergence, the OSPA error remains higher than the proposed method.

B. Intersecting target trajectories with linear constant velocity

As a second example, we consider two targets initially located at $[-1000, 0]^T$ m and $[1000, 0]^T$ m and travelling along linear trajectories with velocities $[30, 30]^T$ m/s and $[-30, 30]^T$ m/s respectively, as shown in Fig. 8. From a multi-target tracking perspective, this represents a more challenging problem, as the tracking filter is faced with a more complicated scenario at the intersection. The corresponding target state estimates obtained using the group sparsity based approach is shown in Fig. 9. Similar to the first example, the estimated target positions are closely grouped around the actual target trajectories throughout the observation period. However, the instantaneous

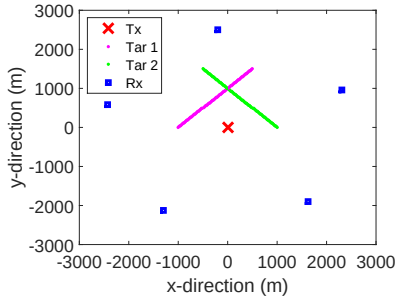

Fig. 8. Intersecting target trajectories with linear constant velocity.

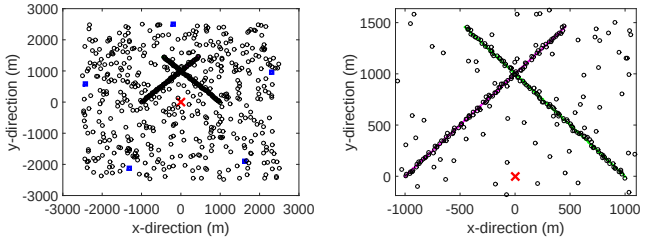

Fig. 9. Instantaneous target state estimation using group sparse reconstruction (a) Entire surveillance area. (b) Enlarged view around the true target trajectories.

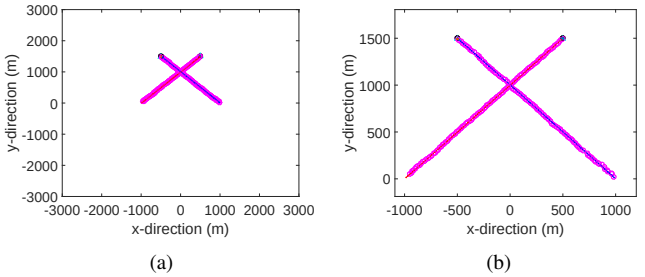

Fig. 10. Results of the GMPHD filter. (a) Entire surveillance area. (b) Enlarged view around the true target trajectories.

target state estimates are subject to missed detections and clutter. It can be observed in Fig. 10 that the filter successfully removes the false measurements, compensates for the missed detections, and reduces the localization error at the steady state. As illustrated in Fig. 11, the proposed method clearly outperforms the random receiver selection based approach in terms of the OSPA error metric. We observe that the proposed method holds a distinct advantage over the random receiver selection based approach for intersecting target trajectories. Around the intersection point at $k = 67$, the proposed method quickly recovers from a small increase in the OSPA error, whereas the performance of the random receiver selection based approach degrades significantly due to the ambiguity in cardinality and also takes a longer recovery period. The proposed method benefits from the accurate instantaneous target state estimates obtained using the CMT-BCS algorithm, which effectively exploits the separation of the targets in a joint position-velocity space.

C. Intersecting target trajectories with nearly-constant velocity

This example represents a scenario with two targets with intersecting trajectories and one of the targets changes its

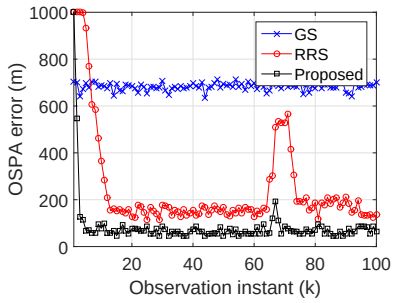

Fig. 11. Performance of the proposed method and the random receiver selection based method for intersecting target trajectories with linear constant velocity.

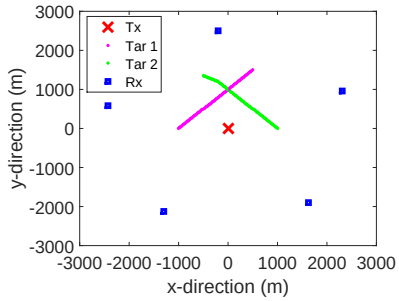

Fig. 12. Intersecting target trajectories with linear nearly-constant velocity.

velocity at some instant during the observation period. We consider two targets initially located at $[-1000, 0]^T$ m and $[1000, 0]^T$ m and travelling along linear trajectories with velocities $[30, 30]^T$ m/s and $[-30, 30]^T$ m/s, respectively, as shown in Fig. 12. The trajectories of the two targets intersect at $k = 67$, and at $k = 81$, the second target changes its trajectory and follows a velocity of $[-30, 15]^T$ m/s. The result of the GMPHD filter corresponding to these instantaneous target state estimates is shown in Fig. 14. Similar to the previous example, the performance of the proposed method degrades momentarily around the intersection point, whereas there is a significant increase in the OSPA error of the random receiver selection based approach, as illustrated in Fig. 15. Likewise, the performance of the proposed method remains robust when the second target changes its trajectory at $k = 81$. The CMT-BCS algorithm yields accurate instantaneous target state estimates irrespective of the change in target trajectory. As such, the nearly-constant velocity model adopted in (2) allows for the slowly changing trajectory, such that the tracking filter accurately follows the gradual change in the true target trajectory, without any significant increase in the OSPA error. However, in the random receiver selection based method, the tracking filter cannot immediately learn about the change in target trajectory from the Doppler frequency measurements, resulting in an increase in the OSPA error.

D. Time-varying number of targets

We consider a scenario with a third target born at $k = 31$ at $[-1200, 1000]^T$ m and travelling along a linear trajectory with a velocity $[20, 20]^T$ m/s in addition to the two targets two targets initially located at $[-1000, 0]^T$ m and $[1000, 0]^T$ m and travelling along linear trajectories with velocities $[30, 30]^T$ m/s and $[-30, 30]^T$ m/s, respectively, as shown in Fig. 16.

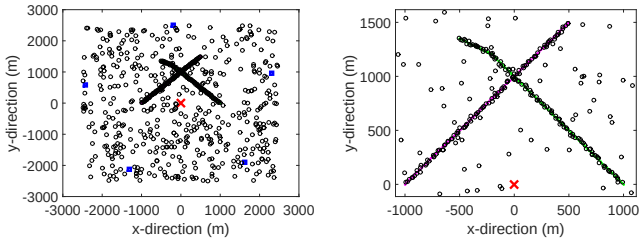

Fig. 13. Instantaneous target state estimation using group sparse reconstruction (a) Entire surveillance area. (b) Enlarged view around the true target trajectories.

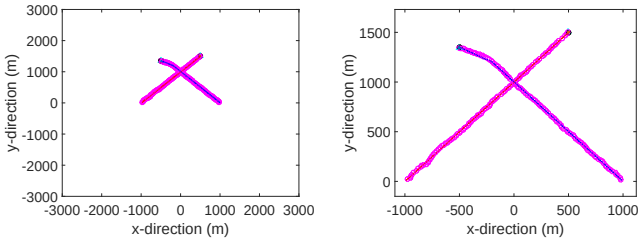

Fig. 14. Results of the GMPHD filter. (a) Entire surveillance area. (b) Enlarged view around the true target trajectories.

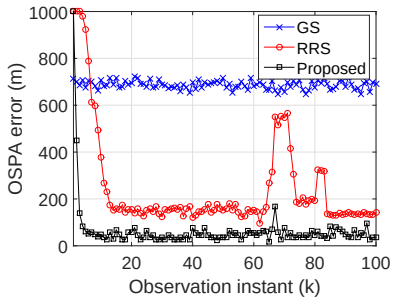

Fig. 15. Performance of the proposed method and the random receiver selection based method for intersecting target trajectories with nearly-constant velocity.

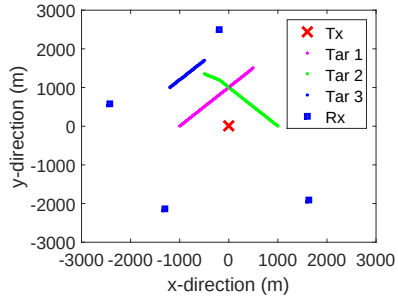

Fig. 16. Intersecting target trajectories with linear nearly-constant velocity.

The trajectories of the two targets intersect at $k = 67$, and at $k = 81$, the second target changes its trajectory and follows a velocity of $[-30, 15]^T$ m/s. The results of the group sparse reconstruction and GMPHD filter corresponding to these trajectories are illustrated in Figs. 17 and 18, respectively. It is evident that the performance of the proposed method degrades for a short period of time when the third target is born at $k = 31$. Nonetheless, it quickly recovers from the change in

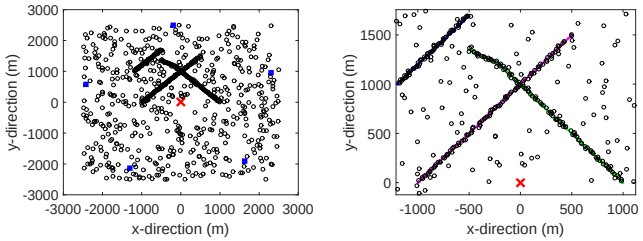

Fig. 17. Instantaneous target state estimation using group sparse reconstruction (a) Entire surveillance area. (b) Enlarged view around the true target trajectories.

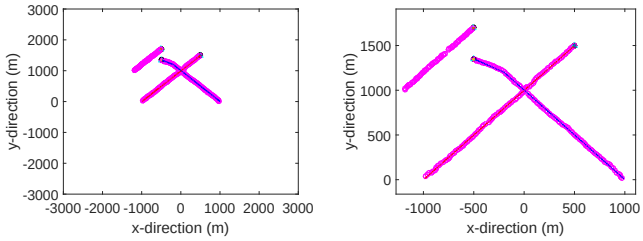

Fig. 18. Results of the GMPHD filter. (a) Entire surveillance area. (b) Enlarged view around the true target trajectories.

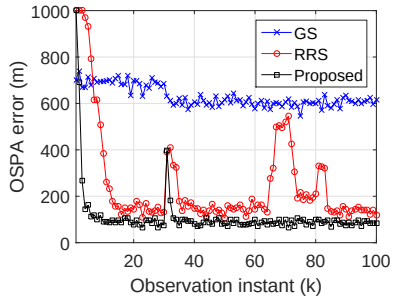

Fig. 19. Performance of the proposed method and the random receiver selection based method for time-varying number of targets.

cardinality and converges to the correct estimation, whereas similar to the previous cases of changes in the trajectories the random receiver selection based approach takes more time to converge, as illustrated in Fig. 19.

VIII. Conclusions

In this paper, we have developed a multi-sensor measurement fusion scheme based on the signal group sparsity shared by all the bistatic links in a discretized position-velocity space for MTT in a PMR system, using Doppler-only measurements. These measurements suffer from single-sensor unobservability, mandating a fusion of measurements from multiple spatially distributed sensors for target state estimation. PMR systems naturally offer measurements from spatially distributed sensors to ensure the required observability. However, data fusion is a computationally intensive problem in multi-sensor multi-target tracking algorithms. In this paper, the instantaneous multi-target state estimates are obtained from group sparse signal reconstruction, which is shown to be an efficient alternative to the existing multi-sensor fusion schemes for MTT algorithms

using Doppler-only measurements. The instantaneous multi-target state estimates are directly fed to the linear Kalman filter-based implementation of the GMPHD filter. Simulation results verified a successful implementation of a multi-target tracking problem in a challenging scenario characterized by noise, false measurements, and uncertain target detections. The performance of the proposed method was validated in different target trajectories using the OSPA error metric and was shown to offer improved performance over the existing random receiver selection based multi-sensor implementation of the GMPHD filter.

REFERENCES

[1] S. Subedi, Y. D. Zhang, M. G. Amin, and B. Himed, "Group sparsity based multi-target tracking in multi-static passive radar systems using Doppler-only measurements," in *Proc. IEEE Int. Radar Conf.*, Arlington, VA, May 2015, pp. 880–885.

[2] J. H. Yoon, D. Y. Kim, S. Bae, and V. Shin, "Joint initialization and tracking of multiple moving objects using Doppler information," *IEEE Trans. Signal Process.*, vol. 59, no. 7, pp. 3447–3452, July 2011.

[3] M. B. Guldogan, D. Lindgren, F. Gustafsson, H. Habberstad, and U. Orguner, "Multi-target tracking with PHD filter using Doppler-only measurements," *Digital Signal Process.*, vol. 27, pp. 1-11, Apr. 2014.

[4] B. Ristic and A. Farina, "Target tracking via multi-static Doppler shifts," *IET Radar, Sonar and Navig.*, vol. 7, no. 5, pp. 508–516, June 2013.

[5] M. Liang, D. Y. Kim, and X. Kai, "Multi-Bernoulli filter for target tracking with multi-static Doppler only measurement", *Signal Process.*, vol. 108, pp. 102–110, Mar. 2015.

[6] G. Battistelli, L. Chisci, S. Morrocchi, F. Papi, A. Farina, and A. Graziano, "Robust multi-sensor multi-target tracker with application to passive multistatic radar tracking," *IEEE Trans. Aerosp. and Electron. Syst.*, vol. 48, no. 4, pp. 3450–3472, Oct. 2012.

[7] J. Shen, A. F. Molisch, and J. Salmi, "Accurate passive location estimation using TOA measurements," *IEEE Trans. Wireless Commun.*, vol. 11, no. 6, pp. 2182–2192, Jun. 2012.

[8] B. Ristic and A. Farina, Alfonso, "Recursive Bayesian state estimation from Doppler-shift measurements," in *Proc. IEEE Int. Conf. Intell. Sensors, Sensor Networks and Info. Process.*, Adelaide, Australia, Dec. 2011, pp. 538–543.

[9] H. D. Griffiths and C. J. Baker, "Passive coherent location radar systems. Part 1: performance prediction," *IEE Proc. - Radar, Sonar and Navig.*, vol. 152, no. 3, pp. 153–159, June 2005.

[10] M. Malanowski, and K. Kulpa, "Two methods for target localization in multi-static passive radar," *IEEE Trans. Aerosp. and Electron. Syst.*, vol. 48, no. 1, pp. 572–580, Jan. 2012.

[11] Y. D. Zhang and B. Himed, "Moving target parameter estimation and SFN ghost rejection in multi-static passive radar," in *Proc. IEEE Radar Conf.*, Ottawa, Canada, Apr. 2013, pp. 1–5.

[12] S. Subedi, Y. D. Zhang, M. G. Amin, and B. Himed, "Robust motion parameter estimation in multi-static passive radar," in *Proc. European Signal Process. Conf.*, Marrakech, Morocco, Sept. 2013, pp. 1–5.

[13] S. Subedi, Y. D. Zhang, M. G. Amin, and B. Himed, "Motion parameter estimation of multiple targets in multi-static radar through sparse signal recovery," in *Proc. IEEE ICASSP*, Florence, Italy, May 2014, pp. 1454-1457.

[14] S. Subedi, Y. D. Zhang, M. G. Amin, and B. Himed, "Motion parameter estimation of multiple ground moving targets in multi-static passive radar systems," *EURASIP J. Adv. Signal Process.*, vol. 2014, no. 157, pp. 1–14, Oct. 2014.

[15] C. R. Berger, S. Zhou, and P. Willett, "Signal extraction using compressed sensing for passive radar with OFDM signals," in *Proc. IEEE FUSION*, Cologne, Germany, July 2008, pp. 1–6.

[16] Y. Bar-Shalom, "Tracking methods in a multitarget environment," *IEEE Trans. Autom. Control*, vol. 23, no. 4, pp. 618–626, Aug. 1978.

[17] M. Mallick, B. N. Vo, T. Kirubarajan, and S. Arulampalam, "Introduction to the issue on multi-target tracking," *IEEE J. Sel. Topics Signal Process.*, vol. 7, no. 3, pp. 373–375, June 2013.

[18] S. S. Blackman, "Multiple hypothesis tracking for multiple target tracking," *IEEE Aerosp. Electron. Syst. Mag.*, vol. 19, no. 1, pp. 5–18, Jan. 2004.

[19] C. Hue, J. P. Le Cadre, and P. Perez, "Tracking multiple objects with particle filtering," *IEEE Trans. Aerosp. Electron. Syst.*, vol. 38, no. 3, pp. 791–812, July 2002.

[20] Y. Bar-Shalom, F. Daum, and J. Huang, "The probabilistic data association filter," *IEEE Control. Syst. Mag.*, vol. 29, no. 6, pp. 82–100, Dec. 2009.

[21] E. W. Kamen, "Multiple target tracking based on symmetric measurement equations," *IEEE Trans. Autom. Control*, vol. 37, no. 3, pp. 371–374, Mar. 1992.

[22] R. P. S. Mahler, "Multitarget Bayes filtering via first-order multitarget moments," *IEEE Trans. Aerosp. Electron. Syst.*, vol. 39, no. 4, pp. 1152–1178, Oct. 2003.

[23] W. F. Leven, and A. D. Lanterman, "Unscented Kalman filters for multiple target tracking with symmetric measurement equations," *IEEE Trans. Autom. Control*, vol. 54, no. 2, pp. 370–375, Feb. 2009.

[24] B. Vo, S. Singh, and A. Doucet, "Sequential Monte Carlo methods for multitarget filtering with random finite sets," *IEEE Trans. Aerosp. Electron. Syst.*, vol. 41, no. 4, pp. 1224–1245, Oct. 2005.

[25] B. Vo and W. K. Ma, "The Gaussian mixture probability hypothesis density filter," *IEEE Trans. Signal Process.*, vol. 54, no. 11, pp. 4091–4104, Nov. 2006.

[26] R. P. S. Mahler, *Statistical Multisource-Multitarget Information Fusion*, Norwood, MA: Artech House, 2007.

[27] B. Vo, B. Vo, R. Hoseinnezhad, and R. P. S. Mahler, "Robust multi-Bernoulli filtering," *IEEE J. Sel. Topics Signal Process.*, vol. 7, no. 3, pp. 399–409, June 2013.

[28] Y. Bar-Shalom and X. Li, *Multitarget-Multisensor Tracking: Principles and Techniques*. New York, NY: YBS, 1995.

[29] E. Mazor, A. Averbuch, Y. Bar-Shalom, and J. Dayan, "Interacting multiple model methods in target tracking: a survey," *IEEE Trans. Aerosp. Electron. Syst.*, vol. 34, no. 1, pp. 103–123, Jan. 1998.

[30] R. P. S. Mahler, " 'Statistics 101' for multisensor, multitarget data fusion," *IEEE Aerosp. Electron. Syst. Mag.*, vol. 19, no. 1, pp. 53–64, Jan. 2004.

[31] R. Mahler, " 'Statistics 102' for multisource-multitarget detection and tracking," *IEEE J. Sel. Topics Signal Process.*, vol. 7, no. 3, pp. 376–389, Jun. 2013.

[32] M. B. Guldogan, D. Lindgren, F. Gustafsson, H. Habberstad, and U. Orguner, "Multiple target tracking with Gaussian mixture PHD filter using passive acoustic Doppler-only measurements," in *Proc. IEEE FUSION*, Singapore, July 2012, pp. 2600–2607.

[33] T. E. Fortmann, Y. Bar-Shalom, and M. Scheffe, "Sonar tracking of multiple targets using joint probabilistic data association," *IEEE J. Ocean. Eng.*, vol. 8, no. 3, pp. 173–184, July 1983.

[34] R. Mahler, "PHD filters of higher order in target number," *IEEE Trans. Aerosp. Electron. Syst.*, vol. 43, no. 4, pp. 1523–1543, Oct. 2007.

[35] R. Mahler, "The multisensor PHD filter: I. General solution via multitarget calculus," in *Proc. SPIE*, vol. 7336, Orlando, FL, Apr. 2009.

[36] B. Shapo and C. Kreucher, "Track-before-fuse error bounds for tracking passive targets," in *Proc. IEEE FUSION*, Chicago, IL, July 2011, pp. 1–8.

[37] C. Kreucher and B. Shapo, "Multitarget detection and tracking using multisensor passive acoustic data," *IEEE J. Ocean. Eng.*, vol. 36, no. 2, pp. 205–218, Apr. 2011.

[38] S. Sun and Z. Deng, "Multi-sensor optimal information fusion Kalman filter," *Automatica*, vol. 40, no. 6, pp. 1017–1023, June 2004.

[39] S. Choi, P. Willet, and S. Zhou, "The PMHT for passive radar in DAB/DVB network," *J. Adv. Inf. Fusion*, vol. 9, no. 1, pp. 27–37, June 2014.

[40] M. Daun, U. Nickel, and W. Koch, "Tracking in multi-static passive radar systems using DAB/DVB-T illumination," *Signal Process.*, vol.

92, no. 6, pp. 1365–1386, June 2012.

[41] N. T. Pham, W. Huang, and S. H. Ong, "Multiple sensor multiple object tracking with GMPHD filter," in *Proc. IEEE FUSION*, Quebec City, Canada, July 2007, pp. 1–7.

[42] D. Schuhmacher, B. T. Ho, and B. N. Ho, "A consistent metric for performance evaluation of multi-object filters," *IEEE Trans. Signal Process.*, vol. 56, no. 8, pp. 3447–3457, Aug. 2008.

[43] B. Ristic, B. Vo, and D. Clark, "Performance evaluation of multi-target tracking using the OSPA metric," in *Proc. IEEE FUSION*, Edinburgh, U.K., July 2010, pp. 1–7.

[44] W. D. Blair, "Design of nearly constant velocity track filters for brief maneuvers," in *Proc. IEEE FUSION*, Chicago, IL, July 2011, pp. 1–8.

[45] D. L. Donoho, "Compressed sensing," *IEEE Trans. Inf. Theory*, vol. 52, no. 4, pp. 1289–1306, Apr. 2006.

[46] C. Rich, "Multitask learning," *Machine Learning*, vol. 28, no. 1, pp. 41–75, Sept. 1997.

[47] Y. C. Eldar, P. Kuppinger, and H. Bolcskei, "Block-sparse signals: uncertainty relations and efficient recovery," *IEEE Trans. Signal Process.*, vol. 58, no. 6, pp. 3042–3054, June 2010.

[48] S. Farahmand, G. B. Giannakis, G. Leus, and Z. Tian, "Sparsity-aware Kalman tracking of target signal strengths on a grid," in *Proc. IEEE FUSION*, Chicago, IL, July 2011, pp. 1–6.

[49] E. Karseras, K. Leung, and W. Dai, "Tracking dynamic sparse signals using Hierarchical Bayesian Kalman filters," in *Proc. IEEE ICASSP*, Vancouver, Canada, May 2013, pp. 6546–6550.

[50] S. Subedi, Y. D. Zhang, and M. G. Amin, "Sparse reconstruction of multi-component Doppler signature exploiting target dynamics," in *Proc. IEEE CAMSAP*, Cancun, Mexico, Dec. 2015, pp. 73–76.

[51] S. Subedi, Y. D. Zhang, M. G. Amin, and B. Himed, "Cramer-Rao type bounds for sparsity-aware multi-target tracking in multi-static passive radar," in *Proc. IEEE Radar Conf.*, Philadelphia, PA, May 2016.

[52] H. W. Lilliefors, "On the Kolmogorov-Smirnov test for normality with mean and variance unknown," *J. American Statist. Assoc.*, vol. 62, no. 318, pp. 399–402, 1967.

[53] E. V. D. Berg and M. Friedlander, "Probing the Pareto frontier for basis pursuit solutions," *SIAM J. Sci. Computing*, vol. 31, no. 2, pp. 890–912, 2008.

[54] M. Yuan and Y. Lin, "Model selection and estimation in regression with grouped variables," *J. Royal Statist. Soc. Series B*, vol. 68, no. 1, pp. 49–67, 2006.

[55] L. Zelnik-Manor, K. Rosenblum, and Y. C. Eldar, "Sensing matrix optimization for block-sparse decoding," *IEEE Trans. Signal Process.*, vol. 59, no. 9, pp. 4300–4312, Sept. 2011.

[56] S. Ji, D. Dunson, and L. Carin, "Multitask compressive sensing," *IEEE Trans. Signal Process.*, vol. 57, no. 1, pp. 92–106, Jan. 2009.

[57] Q. Wu, Y. D. Zhang, M. G. Amin, and B. Himed, "Complex multitask Bayesian compressive sensing," in *Proc. IEEE ICASSP*, Florence, Italy, May 2014, pp. 3375–3379.

[58] B. Ristic, D. Clark, B. Vo, and B. Vo, "Adaptive Target Birth Intensity for PHD and CPHD Filters," *IEEE Trans. Aerosp. Electron. Syst.*, vol. 48, no. 2, pp. 1656–1668, Apr. 2012.

[59] L. Chen, M. J. Wainwright, M. Cetin, and A. S. Willsky, "Multitarget-multisensor data association using the tree-reweighted max-product algorithm." in *Proc. SPIE*, vol. 5096, Orlando, FL, Apr. 2003.

[60] Q. Wu, Y. D. Zhang, M. G. Amin, and B. Himed, "Multi-task Bayesian compressive sensing exploiting intra-task dependency," *IEEE Signal Process. Lett.*, vol. 22, no. 4, pp. 430–434, Apr. 2015.

Saurav Subedi received his M.S. degree in electrical engineering from Missouri University of Science and Technology, Rolla, MO, in 2012. He joined the Center for Advanced Communications, Villanova University, Villanova, PA, in 2012 as a Research Assistant working towards his Ph.D. degree. He joined Bastille Networks, Atlanta, GA, in 2016, where he is currently working as a Data Scientist. His research interests include radar signal processing, sparse signal reconstruction and compressive sensing, and data science.

Mr. Subedi received the Best student Paper Award (Second Place) at the 2015 IEEE International Radar Conference.

Yimin D. Zhang (SM'01) received his Ph.D. degree from the University of Tsukuba, Tsukuba, Japan, in 1988.

Dr. Zhang joined the faculty of the Department of Radio Engineering, Southeast University, Nanjing, China, in 1988. He served as a Director and Technical Manager at the Oriental Science Laboratory, Yokohama, Japan, from 1989 to 1995, a Senior Technical Manager at the Communication Laboratory Japan, Kawasaki, Japan, from 1995 to 1997, and a Visiting Researcher at the ATR Adaptive Communications Research Laboratories, Kyoto, Japan, from 1997 to 1998. He was with the Villanova University, Villanova, PA, USA, from 1998 to 2015, where he was a Research Professor with the Center for Advanced Communications. Since 2015, he has been with the Department of Electrical and Computer Engineering, College of Engineering, Temple University, Philadelphia, PA, USA, where he is currently an Associate Professor. His general research interests lie in the areas of statistical signal and array processing applied for radar, communications, and navigation, including compressive sensing, convex optimization, time-frequency analysis, MIMO system, radar imaging, target localization and tracking, wireless networks, and jammer suppression. He has published more than 290 journal articles and conference papers and 12 book chapters.

Dr. Zhang is a member of the Sensor Array and Multichannel Technical Committee of the IEEE Signal Processing Society. He is an Associate Editor for the *IEEE Transactions on Signal Processing*, and serves on the Editorial Board of the *Signal Processing* journal. He was an Associate Editor for the *IEEE Signal Processing Letters* during 2006–2010, and an Associate Editor for the *Journal of the Franklin Institute* during 2007–2013.

Moeness G. Amin (F'01) received the Ph.D. degree in electrical engineering from the University of Colorado, Boulder, CO, USA, in 1984.

Since 1985, he has been with the Faculty of the Department of Electrical and Computer Engineering, Villanova University, Villanova, PA, USA, where he became the Director of the Center for Advanced Communications, College of Engineering, in 2002. Dr. Amin is a Fellow of the Institute of Electrical and Electronics Engineers; Fellow of the International Society of Optical Engineering; Fellow of the Institute of Engineering and Technology; and Fellow of the European Association for Signal Processing. Dr. Amin is the Recipient of the 2016 Alexander von Humboldt Research Award; Recipient of the 2014 IEEE Signal Processing Society Technical Achievement Award; Recipient of the 2009 Individual Technical Achievement Award from the European Association for Signal Processing; Recipient of the 2015 IEEE Aerospace and Electronic Systems Society Warren D. White Award for Excellence in Radar Engineering; Recipient of the IEEE Third Millennium Medal; Recipient of the 2010 NATO Scientific Achievement Award; Recipient of the 2010 Chief of Naval Research Challenge Award; Recipient of Villanova University Outstanding Faculty Research Award, 1997; and the Recipient of the IEEE Philadelphia Section Award, 1997. He was a Distinguished Lecturer of the IEEE Signal Processing Society, 2003–2004, and is currently the Chair of the Electrical Cluster of the Franklin Institute Committee on Science and the Arts. Dr. Amin has over 700 journal and conference publications in signal processing theory and applications. He co-authored 20 book chapters and is the Editor of the three books *Through the Wall Radar Imaging*, *Compressive Sensing for Urban Radar*, and *Radar for Indoor Monitoring* published by CRC Press in 2011, 2014, and 2017, respectively.

Braham Himed (S'88-M'90-SM'01-F'07) received his Engineer Degree in electrical engineering from Ecole Nationale Polytechnique of Algiers in 1984, and his M.S. and Ph.D. degrees, both in electrical engineering, from Syracuse University, Syracuse, NY, in 1987 and 1990, respectively.

Dr. Himed is a Technical Advisor with the Air Force Research Laboratory, Sensors Directorate, RF Technology Branch, in Dayton, Ohio, USA, where he is involved with several aspects of radar developments. His research interests include detection, estimation, multichannel adaptive signal processing, time series analyses, array processing, adaptive processing, waveform diversity, MIMO radar, passive radar, and over the horizon radar. Dr. Himed is the recipient of the 2001 IEEE region I award for his work on bistatic radar systems, algorithm development, and phenomenology. He is a Fellow of the IEEE and the Vice-Chair of the AESS Radar Systems Panel. He is the recipient of the 2012 IEEE Warren White award for excellence in radar engineering. Dr. Himed is also a Fellow of AFRL (Class of 2013).